Possibility and constraints of ozone friendly working fluids for adsorption refrigeration and gas storage systems

Bidyut Baran SAHA[1,*] Kandadai SRINIVASAN[2] and Kim Choon NG[2]

[1]Department of Mechanical Engineering, Kyushu University
744 Motooka, Nishi-ku, Fukuoka 819-0395, Japan
[2]Department of Mechanical Engineering, National University of Singapore
9 Engineering Drive 1, Singapore 117576

Abstract

The objective of this paper is to consolidate the outcomes of a systematic investigation on the use of adsorption phenomenon for refrigeration and gas storage applications. For refrigeration, thermally powered adsorption cycles based on ozone friendly working fluids working in both partial vacuum and pressurized conditions are considered. The relationships between equilibrium pressures, adsorbent temperatures and equilibrium adsorption concentrations (P-T-W diagram) have been presented. Adsorption uptake data of CO_2 adsorption onto two functional activated carbons are also presented.

Keywords
Adsorption, cooling, refrigeration, thermally powered

Introduction

The quest to accomplish a safe and comfortable environment has always been one of the main preoccupations of the sustainability of human life. Accordingly during the last few decades research aimed at the development of thermally powered adsorption cooling technologies has been intensified. They offer double benefits of reductions in energy consumption, peak electrical demand in tandem with adoption of environmentally benign adsorbent/refrigerant pairs without compromising the desired level of comfort conditions. Alternative adsorption cooling technologies are being developed which can be applied to buildings [1-4]. These systems are relatively simple to construct, as they have no major moving parts. In addition, there is only marginal electricity usage which might be needed for the pumping of heat transfer fluids. The heat source temperature can be as low as 50°C if multi-stage regeneration is implemented [5-6]. A recent study shows that the cooling capacity of the two-stage silica gel/water refrigeration cycle can be improved significantly when a re-heat scheme is employed [7]. However, since the system is driven by low-temperature waste heat, the COP of this thermally activated adsorption systems is normally poor [8]. Another study on micro adsorption hybrid system shows that adsorption and thermoelectric cooling devices can be symbiotically

*Corresponding author: email: saha@mech.kyushu-u.ac.jp, phone: +81-92-802-3101, fax: +81-92-802-3126

combined for use in cooling of computer CPUs [9]. The seemingly low efficiency of each cycle individually is overcome by an amalgamation with the other.

The primary step for developing adsorption refrigeration and gas storage systems is the adsorption performance characterization of the assorted adsorbent-refrigerant pairs. The adsorption parameters enable the derivation of a relationship between uptake, pressure and temperature at equilibrium. The expectations from a specific pair depend on the intended application. Adsorption data are seldom available from the manufacturers. The data from one specimen are not scalable to another. The first objective of this paper is to assess water vapour uptake on various silica gels so as to facilitate selection of the most appropriate system for a given application. The second purpose is to present, five combinations of adsorbent-refrigerant pairs for thermally driven adsorption cooling cycles. Both above and below atmospheric operation are covered. The third aim is to give an overview of adsorption isotherms of two activated carbons andCO_2 which will have implications in not only transcritical CO2 cooling cycles but also in sequestration.

Water vapour uptake of silica gels

The water vapor uptake properties of three different types of silica gels are evaluated using Hydrosorb 1000 analyzer and the pictorial view of the test facility is shown in Fig. 1. The Hydrosorb 1000 offers fully automated, rapid measurement of adsorption and desorption isotherms and evaluation of Brunauer-Emmett-Teller (BET) surface area the and heats of adsorption. Accurate water vapor dosing is made possible by using a unique, heated (100°C) manifold design. Isothermal condition of the adsorbent are attained using a thermal jacket controlled by a constant temperature bath. All the adsorbents are degassed at 140°C for at least 8 hours prior to the experiments to remove any pre-adsorbed moisture.

Fig. 2 compares the water vapor uptake of silica gels at 25°C. The results highlight that at relative pressures > 0.6 the Type-A^{++} silica gel possesses the highest equilibrium uptakes of 537 cc/g followed by Type-A5BW and Type-RD 2560. The inset diagram in Fig. 2 depicts the adsorption and desorption of the water vapor by Type-A^{++} silica gel. However, Type-RD 2650 silica gel exhibits better uptake capacity for lower p/p_0 regions. In adsorption desalination (AD) cycles, p/p_0 is higher since the saline water evaporation temperature is relatively high [10, 11]. This value may get even higher in advanced AD cycle where a number of heat and mass recovery schemes are employed to enhance the production rate.

Adsorption characteristics of activated carbon based adsorption cooling cycles

The Dühring (p-T-W) diagram illustrates the relationship between the pressure, temperature and adsorbate concentration at equilibrium, which can be used to estimate the actual adsorption/desorption processes. In the present study, the Dubinin-Radushkevich (D-R) equation (Eq. 1) is used to predict the adsorption characteristics of ACF (A-15)/ethanol and ACF (A-20)/ethanol [12]. Alternatively, for Chemviron/R134a, Fluka/R134a and Maxsorb II/R134a pairs, Dubinin-Astakhov equation (Eq. 2) is employed therein to predict the adsorption isosters [13].

$$W = W_0 \exp\left\{-\left[RT \ln\left(P_s/P\right)/E\right]^2\right\} \tag{1}$$

$$W = W_0 \exp\left\{-\left[RT \ln\left(P_s/P\right)/E\right]^n\right\}, \tag{2}$$

Figure 1: Pictorial view of the Hydrosorb 1000 analyzer

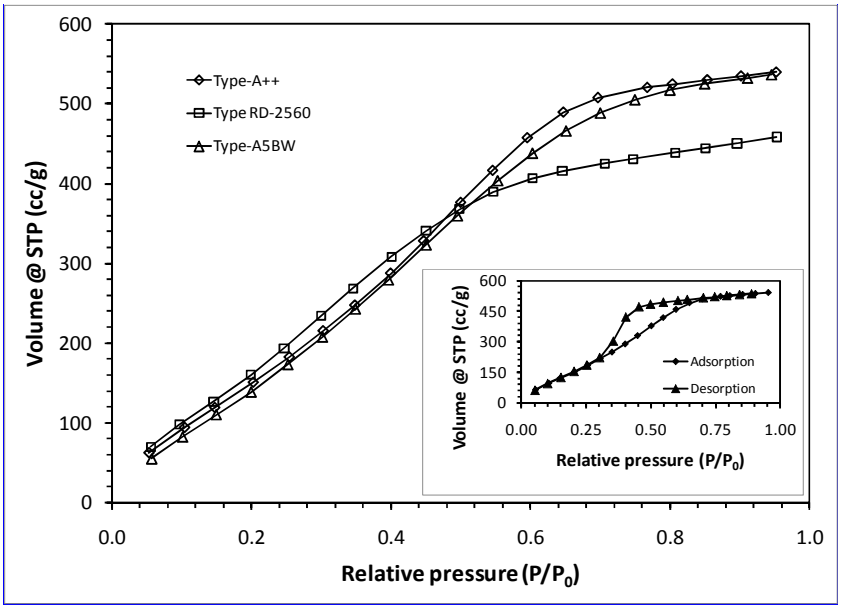

Figure 2: Water vapor uptake by three types of silica gels

In the Dubinin equations, E is the characteristic energy of the adsorbent/adsorbate pair, which can be evaluated from experimental data and R denotes the gas constant. The parameter n is an exponential constant, which provides the best fittings of the experimental isotherms. The term W denotes the specific mass of adsorption or uptake (kg of adsorbate per unit mass of adsorbent) while W_0 is the maximum uptake. The other parameters for D-R and D-A equations are given by El-Sharkawy *et al.* [14]. The single-stage and single-effect double-lift adsorption cooling cycles were superimposed on the Dühring diagram in Fig. 3. The single-stage cycle was represented by the solid lines whereas the single-effect double-lift cycle was represented by doted lines. As can be seen from the idealized Dühring diagram of Fig. 3, the single-effect double-lift cycle can operate with lower heat source temperature as compared to single-stage cooling cycle for the same uptake capacity. Hence, single-effect double-lift cycle is more

preferable for the utilization of low-temperature solar or waste heat sourceswhich is attractive for improving energy conservation and efficiency in cooling purposes.

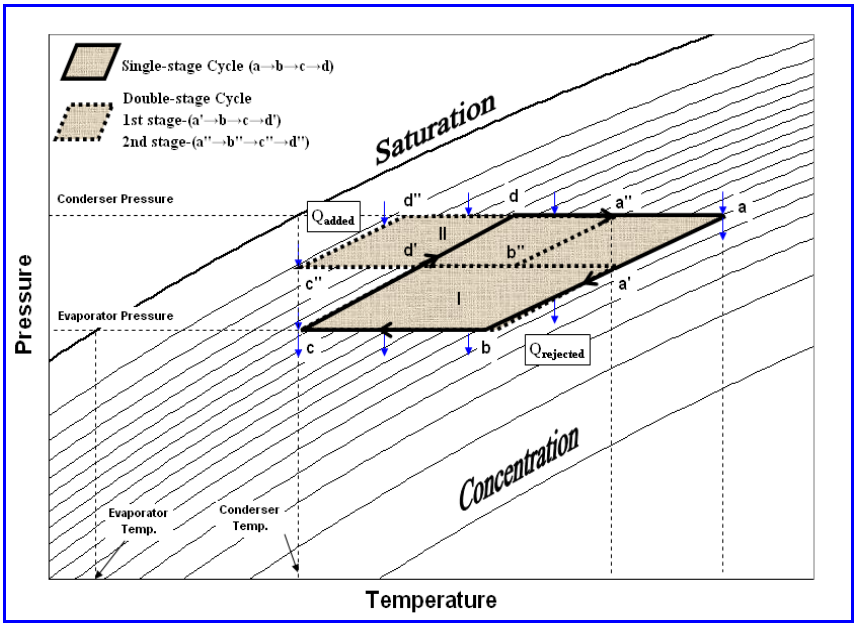

Fig. 3: Qualitative Dühring (P-T-W) diagrams for both single-stage and single-effect double-lift cycles

The ideal adsorption cycle (shown by solid lines in Fig. 3) consists of four sequential thermodynamic processes, i.e. pre-heating (c→d), desorption (d→a), pre-cooling (a→b) and adsorption (b→c) processes. An equilibrium model is adopted to evaluate the cycle performance in term of specific cooling effect (SCE) and coefficient of performance (COP). Being in thermodynamic equilibrium, all the thermal contributions are calculated based on heat and mass balance from the Dühring diagram. The COP of the adsorption cooling cycle is defined as the ratio of the SCE and heat input to the system, Q_h, as shown in Eq. (3). The heat added to the system which is shown in Eq. (4) is simply the summation of both the heat added to the adsorbent (Eq. 5) and refrigerant (Eq. 6). In Eq (5), the specific heat capacities of assorted adsorbents are 900 *J/kg K* for activated carbon fibers and 930 *J/kg* K for other activated carbons. [15, 16] Heat of adsorption is described by Eq. (7) and the function *f(T)* as given in Eq. (8) is deduced through experimental isotherm data for ethanol on activated carbon fiber of types (A-15) and (A-20), HFC-134a on activated carbon powder (Fluka and Maxsorb II) and activated carbon granule (Chemviron) [14].

The specific cooling effect (SCE) is defined as the difference between the evaporator load and heat dissipated to cool the adsorbate from condenser temperature to evaporator temperature, and is shown by Eq. (9).

$$COP = \frac{SCE}{Q_h} \tag{3}$$

$$Q_h = Q_{ads} + Q_{ref} \tag{4}$$

$$Q_{ads} = \int_{T_c}^{T_a} Cp_{ads}\, dT \tag{5}$$

$$Q_{ref} = W_{\max} \int_{T_c}^{T_d} Cp_{ref}\, dT + \int_{T_d}^{T_a} W\, Cp_{ref}\, dT + \int_{W_{\max}}^{W_{\min}} q_{st\ dW} \tag{6}$$

$$q_{st} = h_{fg} + E\left[\ln\left(W_0/W\right)\right]^{1/n} + E \cdot f\left(T\right) \tag{7}$$

$$f\left(T\right) = a\left(T/T_{cri}\right)^b \tag{8}$$

$$SCE = \left(W_{\max} - W_{\min}\right)\left[LH_{T_e} - \int_{T_e}^{T_c} Cp_{ref}\, dT\right] \tag{9}$$

Single-effect double-lift adsorption cycle

The working principle of the single-effect double-lift adsorption cycle has been proposed by Saha *et al.* [17]. The ideal cycle as shown in Fig. 3 by dotted lines, consists of two sequential thermodynamic processes (I and II). These sequential thermodynamic processes employ the same principles as in the single-stage single-lift cooling cycle, at which the pre-heating, desorption, pre-cooling and adsorption processes for the first and second stages are indicated as c→d′→a′→b and c″→d″→a″→b″, respectively. In the single-effect double-lift adsorption cycle, there is an additional pair of adsorbent beds incorporated in between the evaporator and condenser of the system. These extra adsorbent beds allow the refrigerant pressure to increase from evaporator to condenser in two stages. At the same time, this enables the single-effect double-lift cycle to reduce the regeneration temperature of the adsorption cycle utilising a two stage pressure reduction between the condenser and evaporator. In the present simulation, the total mass of adsorbent for single-stage cycle is assumed to be equal to single-effect double-lift cycle, implying that each bed in the single-effect double-lift cycle will carry only half the amount of adsorbent as the adsorbent bed in single-stage adsorption cycle. The simulated performances of single-effect double-lift adsorption cycle are compared with the single-stage adsorption cycle in terms of COP and SCE.

Simulations for the five assorted working pairs [ACF (A-15)/ethanol, ACF (A-20)/ethanol, Chemviron/R134a, Fluka/R134a and Maxsorb II/R134a) are carried out at partial vacuum (for ethanol) and pressurized conditions (for R134a). The working pressures for ACF (A-15)/ethanol and ACF (A-20)/ethanol are between 1~10 kPa. The Chemviron/R134a, Fluka/R134a and Maxsorb II/R134a based pressurized adsorption cycles are operated for pressure between 300~800 kPa. These pressures are calculated from the saturation pressures at the evaporator and condenser temperatures.

Table 1 below shows the temperature data at pre-cooling, adsorption, pre-heating and desorption processes for both the single-stage and single-effect double-lift cycles of the five pairs. The uptakes (W) of these pairs are simulated from Eq. (1) and Eq. (2). For the same amount of uptake capacity ($\Delta W = W_{max}-W_{min}$), single-effect double-lift cycles require lower desorption or regeneration temperatures, T_g compared to those of the single-stage cycle. For instant, Maxsorb II-R134a working pair at uptake capacity of 0.36 kg/kg, the T_g at single-stage and single-effect double-lift cycles are equal to 80 ºC and 67 ºC, respectively. Among these working pairs, Maxsorb II/R134a has the highest uptake capacity which is followed

respectively by ACF (A-20)/ethanol, ACF (A-15)/ethanol, Fluka/R134a and Chemviron/R134a pairs.

Table 1: Adsorbent temperature and uptake capacity for idealized adsorption/desorption cycle simulated at T_{evap} = 6.7°C and T_{cond} = 29.4°C in accordance to ARI Standard 560. The subscripts correspond to thermodynamic state points in Fig. 3.

				Adsorbent/refrigerant pairs				
				ACF (A-15)/ ethanol	ACF (A-20)/ ethanol	Chemviron/ R134a	Fluka/ R134a	Maxsorb II/ R134a
Single-stage cycle		Temperature [°C]	T_a	80	80	80	80	80
			T_b	52	52	53	53	53
			T_c	30	30	30	30	30
			T_d	55	55	55	55	55
		Uptake [kg/kg]	W_{min}	0.28	0.25	0.31	0.36	1.39
			W_{max}	0.47	0.58	0.34	0.45	1.75
			ΔW	0.19	0.33	0.03	0.09	0.36
single-effect double-lift cycle	1st Cycle	Temperature [°C]	T_a'	66	66	63	67	67
			T_b	52	52	50	53	53
			T_c	30	30	30	30	30
			T_d'	42	42	42	42	42
		Uptake [kg/kg]	W_{min}	0.28	0.25	0.31	0.36	1.39
			W_{max}	0.47	0.58	0.34	0.45	1.75
			ΔW	0.19	0.33	0.03	0.09	0.36
	2nd Cycle	Temperature [°C]	T_a''	66	66	63	67	67
			T_b''	52	52	50	53	53
			T_c''	30	30	30	30	30
			T_d''	42	42	42	42	42
		Uptake [kg/kg]	W_{min}	0.39	0.43	0.33	0.40	1.58
			W_{max}	0.58	0.76	0.36	0.49	1.94
			ΔW	0.19	0.33	0.03	0.09	0.36

Table 2 summarizes the effect of regeneration temperature on the COP and SCE of single-stage and single-effect double-lift cycles. It is evident that the SCE values increase linearly with regeneration temperature for all five pairs. For both single-stage and single-effect double-lift cycles, ACF (A-20)/ethanol provides the highest value for SCE which is followed by ACF (A-15)/ethanol, Maxsorb II/R134a, Fluka/R134a and lastly Chemviron/R134a. Generally the sub-atmospheric systems possess higher SCE and COP than pressurized systems.

Table 2: COP and SCE for single and two-stages ideal adsorption cooling cycle, simulated at same conditions of Table 1 [18].

		Adsorbent/refrigerant pairs	Regeneration Temperature [ºC]								
			45	50	55	60	65	70	75	80	85
Single stage cycle	COP	(A-15)/Ethanol	-	-	0.05	0.30	0.42	0.49	0.53	0.55	0.56
		(A-20)/Ethanol	-	-	0.08	0.42	0.56	0.62	0.65	0.67	0.68
		Chemviron/R134a	-	-	0.01	0.02	0.03	0.04	0.05	0.06	0.06
		Fluka/R134a	-	-	0.01	0.06	0.10	0.12	0.14	0.15	0.15
		Maxsorb II/R134a	-	-	0.02	0.09	0.14	0.18	0.20	0.22	0.23
	SCE [kJ/kg_ads]	(A-15)/Ethanol	-	-	2.92	29.0	63.7	99.7	135.9	171.2	205.0
		(A-20)/Ethanol	-	-	5.85	56.8	121.6	184.8	243.8	297.2	344.0
		Chemviron/R134a	-	-	0.13	0.83	1.75	2.71	3.72	4.75	5.82
		Fluka/R134a	-	-	0.56	3.28	6.50	9.53	12.4	15.1	17.7
		Maxsorb II/R134a	-	-	1.83	11.2	23.0	34.7	46.4	57.9	69.3
single-effect double-lift Cycle	COP	(A-15)/Ethanol	0.06	0.11	0.13	0.14	0.15	0.15	0.16	0.16	0.16
		(A-20)/Ethanol	0.11	0.16	0.17	0.18	0.18	0.18	0.19	0.19	0.19
		Chemviron/R134a	0.01	0.01	0.01	0.02	0.02	0.02	0.02	0.02	0.02
		Fluka/R134a	0.02	0.04	0.04	0.05	0.05	0.05	0.05	0.05	0.05
		Maxsorb II/R134a	0.02	0.05	0.06	0.06	0.07	0.07	0.07	0.07	0.07
	SCE [kJ/kg_ads]	(A-15)/Ethanol	5.64	17.7	32.2	48.6	66.2	84.5	102.9	120.9	138.1
		(A-20)/Ethanol	15.3	50.3	85.0	117.8	147.6	173.7	195.8	213.8	228.2
		Chemviron/R134a	0.20	0.58	1.00	1.45	1.93	2.43	2.95	3.49	4.05
		Fluka/R134a	0.94	2.84	4.61	6.28	7.85	9.33	10.7	12.1	13.3
		Maxsorb II/R134a	3.16	8.99	15.0	21.0	27.2	33.3	39.4	45.4	51.3

Adsorption isotherms of Carbon dioxide on activated carbons

The adsorption isotherms of CO_2 on Maxsorb III and ACF (A-20) have been conducted using volumetric technique for temperatures ranging from -18 to 80 °C and pressures up to 10 MPa. Fig. 4 shows a schematic diagram of the experimental apparatus, which comprises; (i) adsorption and loading cells designed to stand pressure of 12 MPa, (ii) two water baths connected with two water circulators, and (iii) a 25.8 μm mesh attached at the center of adsorption cell to aid faster adsorption. The adsorption cell is connected to the loading cell through 1/4" stainless steel pipe and a set of Swagelok fittings. Other parts are stopping valves, safety valves, and 15 μm pore size filter. Tape heaters are mounted on tubes shown by zigzag lines in Fig. 4 to control their temperatures.

Data reduction

The primary data are the loading pressure p_l, the equilibrium pressure p_{eq}, the loading cell temperature T_l and adsorbent temperature T_a. The mass adsorbed in the nth measurement can be determined by Eq. (10) below, where n varies from 1 to 7.

$$m_n = m_{n-1} + \Delta m_{load,n} - \Delta m_{void,n} \qquad (10)$$

where, m_{n-1} is the previous amount adsorbed, $\Delta m_{load,n}$ is the mass difference in the loading cell between loading and equilibrium states and $\Delta m_{void,n}$ is the mass added to the void volume.

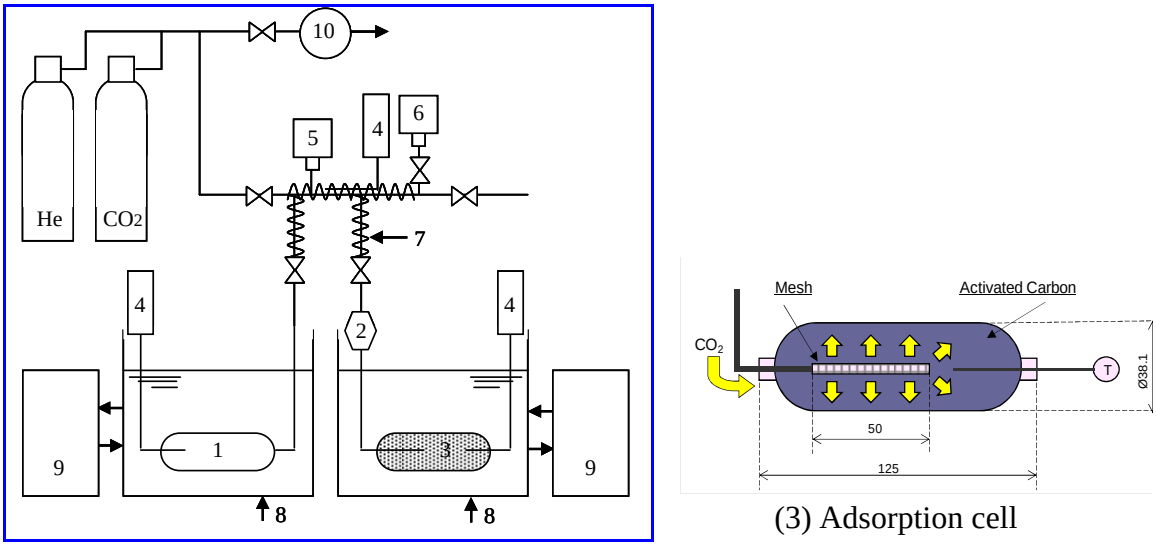

Fig. 4: Schematic diagram of volumetric experimental apparatus. (1: loading cell, 2: filter, 3: adsorption cell (details shown in the right), 4: thermocouple, 5: pressure transducer 6: vacuum gauge, 7: tape heaters, 8: water bath, 9: water circulator, 10: vacuum pump).

Correlation of isotherms:

The experimental data are fitted with the Langmuir, Tóth, Dubinin-Astakhov (D-A) and modified D-A isotherm equations. A nonlinear optimization routine is used to optimize the parameters of these models to fit the experimental data for multiple temperatures. The well-known Langmuir and Tóth isotherm models can be expressed by Eqs. (11) and (12), respectively [19].

$$\frac{C}{C_0} = \frac{bP}{1+bP} \tag{11}$$

$$\frac{C}{C_0} = \frac{bP}{\left(1+(bP)^t\right)^{\frac{1}{t}}} \tag{12}$$

where C/kg·kg^{-1} is the amount adsorbed, C_0/kg·kg^{-1} is the saturated amount adsorbed, P/MPa the equilibrium pressure and b/MPa^{-1} the adsorption affinity given by:

$$b = b_0 e^{\left(\frac{Q}{RT}\right)} \tag{13}$$

where b_0 is the adsorption affinity at infinite temperature and Q is the isosteric heat of adsorption. The parameter t in Eq. (12) is known to characterize the system heterogeneity. The lower the value of t, the more heterogeneous is the system. If t is equal to unity, Tóth isotherm is reduced to the Langmuir isotherm.

For the Dubinin-Astakhov model Eq. (2) is used and a modified D-A model where the estimation of pseudo-vapor pressures takes into account the interactions between adsorbate-adsorbent system and is given by [20] as:

$$P_s = \left(\frac{T}{T_c}\right)^k P_c \tag{14}$$

where k is a constant obtained from the fitting of experimental adsorption isotherm data. For CO_2 adsorption on ACF (A-20) and Maxsorb III, *k* is found to be 3.86 and 4.49, respectively.
The experimental uptake curves of CO_2 onto ACF (A-20) and Maxsorb III for temperatures ranging from (-18 to 80) ºC and pressures up to 10 MPa are shown in Figs. 5 and 6, respectively. The shape of the adsorption isotherms of CO_2 in the assorted micro-porous materials is monotonically concave and therefore can be classified as type I in the IUPAC classification [21]. As can be seen from Figs. 5 and 6, the maximum uptake of CO_2 onto ACF (A-20) near the saturation pressure is 1 kg CO_2 per kg of ACF (A-20) and that of CO_2 onto Maxsorb III is 1.7 kg of CO_2 per kg of Maxsorb III. In both cases, each experimental point is found within ± 5 % deviation with the Tóth model.

The fitting parameters of the D-A and modified D-A equations for the adsorption of CO_2 onto ACF (A-20) and Maxsorb III are presented in Table 3. The D-A equation yields *RMSDs* as high as 6.61 % for ACF (A-20) and 9.58 % for Maxsorb III. However, the use of the modified D-A equation reduces the RMSD as low as 3.58 % and 4.53 % for ACF (A-20) and Maxsorb III, respectively. The root mean square deviation (RMSD) between the calculated values (cal) and experimental data (exp) is defined as:

$$RMSD = \sqrt{\frac{\sum_0^N \left(\frac{C_{\exp} - C_{cal}}{C_{\exp}} \cdot 100\right)^2}{N}} \tag{15}$$

Table 3: Fitting parameters of D-A and modified D-A models for CO_2 adsorption onto ACF (A-20) and Maxsorb III.

Adsorbent	Model	*k*	W_0/ $cm^3 \cdot g^{-1}$	E/J·mol^{-1}	*n*	*RMSD*
A-20	D-A	2	1.002	4468.22	1.14	6.61
	Modified D-A	3.86	1.03	4549.92	1.18	3.58
Maxsorb III	D-A	2	1.727	3983.24	1.12	9.58
	Modified D-A	4.49	1.759	4159.89	1.18	4.53

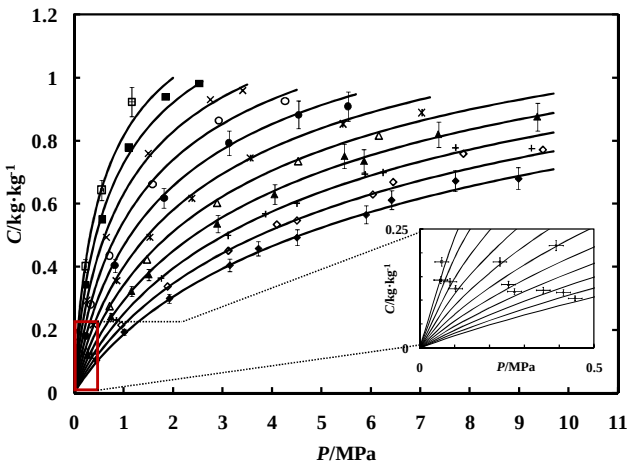

Fig. 5: Adsorption isotherm of CO_2 on ACF (A-20) with ± 5 % error bars in uptake and ± 0.02 MPa horizontal error bars in pressure: □, -18.8 °C; ■, -10 °C; ×, 0 °C; ○, 10 °C; ●, 20 °C; *, 30 °C; Δ, 40 °C; ▲, 50 °C; +, 60 °C; ◊, 70 °C; ♦, 80 °C; solid lines are from the Tóth model [22].

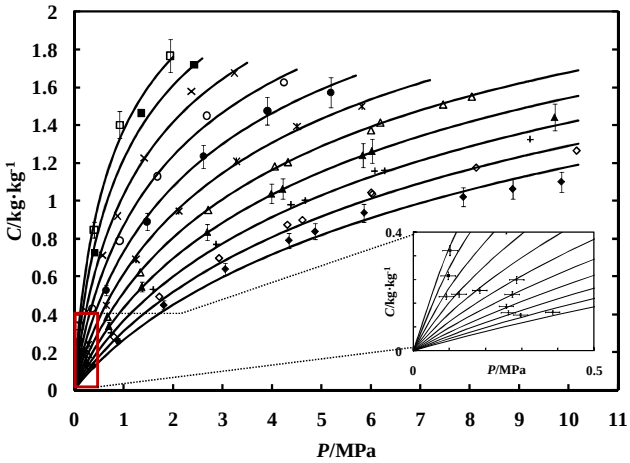

Fig. 6: Adsorption isotherm of CO_2 on Maxsorb III with ± 5 % error bars in uptake and ± 0.02 MPa horizontal error bars in pressure: □, -17.6 °C; ■, -10 °C; ×, 0 °C; ○, 10 °C; ●, 20 °C; *, 30 °C; Δ, 40 °C; ▲, 50 °C; +, 60 °C; ◊, 70 °C; ♦, 80 °C; solid lines are from the Tóth model [22].

Concluding remarks

The salient points of the present study are summarized as follows:

(a) The water vapor uptake analysis reveals that RD type silica gel-water pair seems to be the most suitable for adsorption cooling applications. Type-A^{++} silica gel is the best choice for adsorption desalination application where the p/p0 is relatively high due to higher saline water evaporation temperature conditions.

(b) ACF (A-20)/ethanol pair provides the highest value of specific cooling effect.

(c) Partial-vacuum adsorption cooling cycles provide better COP and SCE than pressurized cycles at the same operating temperature conditions.

(d) At relatively lower regeneration temperature (less than 70°C), the single-effect double-lift cycle provides higher specific cooling effect. Single-stage cycles attain higher COP values than those of single-effect double-lift cycles at relatively higher heat source temperatures.

(e) Adsorption isotherm data for CO_2 on ACF (A-20) and Maxsorb III are presented in -18 to 80°C temperature range and pressures up to 10 MPa. The data have been successfully correlated to popular isotherm equations within ± 5 % uncertainty. Adsorption uptake of CO_2 on Maxsorb III is about 1.7 times higher than that of ACF (A-20). CO_2 adsorption data can be used for CO_2 sequestration.

(f) The main direction for future research work on adsorbent-refrigerant pairs is related to the development of functional adsorbents with high heat and mass transfer performance. Another direction for future research work is the search for environment friendly working pairs that could be powered by low-temperature heat source.

References

[1] Saha B.B., Boelman E., Kashiwagi T., 1995, "Computer simulation of a silica gel water adsorption refrigeration cycle - the influence of operating conditions on cooling output and COP", *ASHRAE Transactions*, Vol. 101, No. 2, pp. 348-357.

[2] Boelman E., Saha B.B., Kashiwagi T., 1995, "Experimental investigation of a silica gel water adsorption refrigeration cycle - the influence of operating conditions on cooling output and COP", *ASHRAE Transactions*, Vol. 101, No. 2, pp. 358-366.

[3] Zhai X.Q., Wang R.Z., 2009, "Experimental investigation and theoretical analysis of the solar adsorption cooling system in a green building", *Applied Thermal Engineering*, Vol. 20, No. 1, pp. 17-27.

[4] Grisel R.J.H., Smeding S.F., de Boer R., 2010, "Waste heat driven silica gel/water adsorption cooling in trigeneration", *Applied Thermal Engineering*, Vol. 30, Nos. 8-9, pp. 1039-1046.

[5] Saha B.B., Akisawa A., Kashiwagi T., 2001, "Solar/waste heat driven two-stage adsorption chiller: the prototype", *Renewable Energy*, Vol. 23, No. 1, pp. 93-101.

[6] Saha B.B., Chakraborty A., Koyama S., Srinivasan K., Ng K.C., Kashiwagi T., Dutta P., 2007,"Thermodynamic formalism of minimum heat source temperature for driving advanced adsorption cooling device", *Applied Physics Letters*, Vol. 91, 111902.

[7] Alam K.C.A., Khan M.Z.I., Uyun A.S., Hamamoto Y., Akisawa A., Kashiwagi T., 2007, "Experimental study of a low temperature heat driven re-heat two-stage adsorption chiller", *Applied Thermal Engineering*, Vol. 27, No. 10, pp. 1686-1692.

[8] Saha B.B., Koyama S., Kashiwagi T., Akisawa A., Ng K.C., Chua H.T., 2003, "Waste heat driven dual-mode, multi-stage, multi-bed regenerative adsorption system", *International Journal of Refrigeration*, Vol. 26, No. 7, pp. 749-757.

[9] Saha B.B., Chakraborty A., Koyama S., Ng K.C., Sai M.A., 2006, "Performance modelling of an electro-adsorption chiller", *Philosophical Magazine*, Vol. 86, No. 23, pp. 3613-3632.

[10] Ng K.C., Thu K., Yanagi H., Saha B.B., Chakraborty A., Al-Ghasham T.Y., 2009, "Apparatus and Method for Improved Desalination", PCT/SG2009/000223, WO 2009/157875.

[11] Thu K., Ng K.C., Saha B.B., Chakraborty A., Koyama S., 2009, "Operational strategy of adsorption desalination system", *International Journal of Heat and Mass Transfer*, Vol. 52, Nos. 7-8, pp. 1811-1816.

[12] El-Sharkawy I.I., Kuwahara K., Saha B.B., Koyama S., Ng K.C., 2006, "Experimental investigation of activated carbon fibers/ethanol pairs for adsorption cooling system application", *Applied Thermal Engineering* Vol. 26, Nos. 8-9, pp. 859-865.

[13] Banker N.D., Srinivasan K., Prasad M., 2004, "Performance analysis of activated carbon + HFC-134a adsorption coolers", *Carbon* Vol. 42, No. 1, Pp. 117-127.

[14] El-Sharkawy I.I., Saha B.B., Koyama S., Srinivasan K., 2007, "Isosteric heats of adsorption extracted from experiments of ethanol and HFC-134a on carbon based adsorbents", *International Journal of Heat and Mass Transfer*, Vol. 50, Nos. 5-6, Pp. 902-907.

[15] Yeung K.H., Sumathy K., 2003, "Thermodynamic analysis and optimization of a combined adsorption heating and cooling system", *International Journal of Energy Research*, Vol. 27, No. 15, pp. 1299-1315.

[16] Wang L.W., Wang R.Z., Lu Z.S., Chen C.J., Wang K., Wu J.Y., 2006, "The performance of two adsorption ice making test units using activated carbon and a carbon composite as adsorbents", *Carbon*, Vol. 44, No. 13, pp. 2671-2680.

[17] Saha B.B., Koyama S., Ng K.C., Hamamoto Y., Akisawa A., Kashiwagi T., 2006, "Study on a dual-mode, multi-stage, multi-bed regenerative adsorption chiller", *Renewable Energy*, Vol. 31, No. 13**,** pp. 2076-2090.

[18] Loh W.S., El-Sharkawy I.I.,' Ng K.C., Saha B.B., 2009, "Adsorption cooling cycles for alternative adsorbent/adsorbate pairs working at partial vacuum and pressurized conditions", *Applied Thermal Engineering*, Vol. 29, No. 4, pp. 793-798.

[19] Do D.D., 1998, "Adsorption Analysis: Equilibria and Kinetics", Series in Chemical Engineering, Imperial College Press, London.

[20] Amankwah K.A.G., Schwarz J.A.A., 1995, "Modified approach for estimating pseudo-vapor pressures in the application of the Dubinin-Astakhov equation", *Carbon*, Vol. 33, pp. 1313-1319.

[21] Sing K.S.W., Everett D.H., Haul R.A.W., Moscoul L., Pierotti R.A., Rouqerol J., Siemieniewska T., 1985, "Reporting physisorption data for gas/solid systems with special reference to the determination of surface area and porosity", *Pure Appl. Chem.* Vol. 57, pp. 603−619.

[22] Saha B.B., Jribi S., Koyama S., El-Sharkawy I.I., 2011, "Carbon dioxide adsorption isotherms on activated carbons", *Journal of Chemical and Engineering Data*, je-2010-00973t, in press.